

Role of initial conditions in spin-glass aging experimentsV. S. Zotev, G. F. Rodriguez, G. G. Kenning, and R. Orbach
Department of Physics, University of California, Riverside, California 92521

E. Vincent and J. Hammann

Service de Physique de l'Etat Condense, CEA Saclay, 91191 Gif-sur-Yvette Cedex, France

(Received 22 February 2002; revised manuscript received 3 March 2003; published 30 May 2003)

The effect of initial conditions on aging properties of the spin-glass state is studied for a single crystal Cu:Mn 1.5 at %. It is shown that the memory of the initial state, created by the cooling process, remains strong on all experimental time scales. The t/t_w scaling properties of two relaxation functions, the thermoremanent magnetization (TRM) and the isothermal remanent magnetization (IRM) (with $t_{w1}=0$ and $t_{w2}=t_w$), are compared in detail. It is observed that the IRM relaxation as a function of t/t_w demonstrates a superaging behavior. This result suggests that the subaging, exhibited by the TRM decay, arises from the influence of the cooling process, and cannot be considered a natural type of scaling in spin-glass dynamics.

DOI: 10.1103/PhysRevB.67.184422

PACS number(s): 75.50.Lk, 75.40.Gb

I. INTRODUCTION

Aging phenomena in spin glasses have been studied for 20 years.¹ Despite considerable progress, some problems remain open. One of them is the problem of t/t_w scaling of time dependent quantities.² This issue is a touchstone in our understanding of spin-glass dynamics. Only when all departures from full t/t_w scaling are accounted for, both theoretically and experimentally, can one say that the aging phenomena are well understood.

A waiting time t_w between the end of a cooling process and a change in magnetic field is a natural scaling parameter, because it is the only externally defined time scale. However, the existence of this characteristic time scale does not necessitate a full t/t_w scaling of two-time quantities. In fact, various departures from the full scaling are more common than the t/t_w scaling itself. The lack of scaling may have different reasons, and no theoretical approach at present can take them all into account. Therefore, we begin this paper with a brief review of the main experimental and theoretical results on t/t_w scaling.

First experimental results on time scaling of the thermoremanent magnetization (TRM) were obtained soon after the aging effects were discovered. They demonstrated that there are small but systematic deviations from full t/t_w scaling in the aging regime.^{3,4} It was shown that the TRM curves for different waiting times can be successfully superimposed if a power of the waiting time, t_w^μ , with $\mu < 1$, is used in the analysis instead of the actual t_w . This phenomenon is often referred to as “subaging”: the apparent age of the spin-glass state, determined from the scaling of the TRM curves, increases slower than the waiting time t_w . The t/t_w^μ scaling was first used in studies of physical aging in polymer mechanics.⁵ The spin-glass aging experiments also suggested^{3,4} that t_w -independent quasiequilibrium relaxation at short observation times should be taken into account properly, if a good scaling over a wide time range is to be achieved. Nevertheless, a full t/t_w scaling in the aging regime was never derived from experimental data. Departures

of μ from unity are small, but persistent.² Physical meaning of this scaling parameter remains unclear even though different interpretations have been proposed.^{6,7} All this suggests that there may be some additional reasons for the lack of scaling, which have not been taken into account yet.

On the theoretical side, the situation is more ambiguous. Phenomenological phase-space models,^{8,9} describing aging as thermally activated hopping over free-energy barriers, suggest a full t/t_w scaling in the absence of finite-size effects. In the mean-field dynamics, however, two different cases are distinguished.¹⁰ Those mean-field models, in which one level of replica-symmetry breaking is exact (like the spherical p -spin model), have only one time scale in the aging regime, and a full t/t_w scaling may be expected.¹¹ Models with continuous replica-symmetry breaking (like the Sherrington-Kirkpatrick model), are characterized by an infinite number of relaxation time scales.¹² If a decay of the correlation function in the aging regime is viewed as a sequence of infinitesimal steps, then each step takes much longer than the previous one.¹³ Therefore, no t/t_w scaling is expected in these models. It is suggested^{10,13} that full t/t_w scaling for all times in the aging regime would rule out the continuous replica-symmetry breaking scenario.

The phenomenological droplet model,¹⁴ which assumes that free-energy barriers grow as a power law of the droplet size, $B \propto L^\psi$, suggests the logarithmic scaling, $\ln(t)/\ln(t_w)$, in the long-time limit. It has been argued,¹⁵ however, that algebraic relaxation with t/t_w scaling can be predicted within this model, if one assumes a modified scaling law for the energy barriers: $B \propto \ln(L)$.

Theoretical studies also show that the aging dynamics of some models are characterized by logarithmic corrections.^{16,17} Depending on the nature of these corrections, a full t/t_w scaling may¹⁶ or may not¹⁷ be asymptotically recovered in the long-time limit.

These theoretical results suggest that it would be naive to analyze experimental data with a firm belief that they should (“ideally”) exhibit a full t/t_w scaling. At the same time, a reliable experimental evidence of the presence (or absence) of such scaling would be very important, because it might

help to determine the validity of different theoretical pictures.

Many experimental and theoretical studies of aging dynamics in spin glasses have one thing in common: they focus entirely on the aging phenomena, and neglect possible cooling effects. We argue in the present paper that one of the reasons for the lack of a full t/t_w scaling in spin-glass aging experiments is the influence of the cooling process. Our line of argument is the following. A typical spin-glass relaxation experiment includes cooling from above the glass temperature.¹⁸ The approach of the measurement temperature is necessarily slow with possible oscillations, because the temperature has to be stabilized. Temperature cycling experiments,^{19–21} as well as aging experiments with different cooling rates,²² have shown that the thermal history near the measurement temperature has a profound effect on the subsequent spin-glass behavior. Any aging experiment is, therefore, a temperature variation experiment, and properties of the measured relaxation are determined by both cooling and waiting time effects. As the waiting time increases, the influence of the initial condition, set by the cooling process, diminishes. This may lead to systematic departures from full t/t_w scaling, compatible with the experimentally observed behavior.

The paper is organized as follows. Section II discusses general properties of spin-glass relaxation and methods for analysis of t/t_w scaling. In Sec. III A, features of the cooling process and properties of the TRM decay for $t_w=0$ are studied. In Sec. III B, t/t_w scaling properties of the TRM and the isothermal remanent magnetization (IRM) are compared in detail. In Sec. III C, our experimental results are discussed in comparison with results of numerical simulations. Section IV summarizes our arguments.

II. THEORETICAL BACKGROUND

A. Linear response in spin glasses

In a typical TRM experiment, a spin-glass sample is cooled down from above the glass temperature T_g to a measurement temperature $T < T_g$ in the presence of a small magnetic field h . It is then kept at the measurement temperature during the waiting time t_w . After that, the field h is cut to zero, and a decay of the TRM is measured as a function of the observation time t , elapsed after the field change. This decay depends on the waiting time—a phenomenon called aging. The total age of the system is $t + t_w$. In a more complex IRM protocol, the sample is cooled down at zero magnetic field and kept for a waiting time t_{w1} . Then a small magnetic field is turned on, and, after an additional waiting time t_{w2} , is turned off again. A subsequent decay of the isothermal remanent magnetization is observed. It depends on both waiting times.

In order to describe time evolution of a system, the auto-correlation function $C(t_1, t_2)$ is introduced:

$$C(t_1, t_2) = (1/N) \sum_{i=1}^N \langle S_i(t_1) S_i(t_2) \rangle. \quad (1)$$

It depends on two times, t_1 and t_2 , measured from the end of the cooling process. The response of the system at time t_1 to an instantaneous field h , present at time t_2 , is described by the response function:

$$R(t_1, t_2) = (1/N) \sum_{i=1}^N \delta \langle S_i(t_1) \rangle / \delta h(t_2). \quad (2)$$

In thermal equilibrium, both functions depend only on the time difference, $t_1 - t_2$. They are related by the fluctuation-dissipation theorem. If the system is out of equilibrium, the following generalization of this theorem is expected to hold in the long-time limit¹⁰:

$$R(t_1, t_2) = \beta X[C] \partial C(t_1, t_2) / \partial t_2. \quad (3)$$

Here $\beta = 1/k_B T$, and $X[C]$ is the fluctuation-dissipation ratio, which is equal to unity in equilibrium. It is suggested^{10–12} that, for long waiting times, X depends on its time arguments only through the correlation function, i.e., $X(t_1, t_2) = X[C(t_1, t_2)]$, as specified in Eq. (3).

The magnetic susceptibility, measured in spin-glass experiments, is an integrated response. If a magnetic field is applied at time $t' = 0$ and removed at $t' = t_w$, the susceptibility, measured at the observation time t , is given by the following expression:

$$\chi_{IRM}(t + t_w, t_w) = \int_0^{t_w} R(t + t_w, t') dt'. \quad (4)$$

This corresponds to the IRM experimental protocol with $t_{w1} = 0$ and $t_{w2} = t_w$. In what follows, the notation IRM will always refer to the isothermal remanent magnetization with $t_{w1} = 0$, which is a two-time quantity. Using Eq. (3) for the response function and introducing a function $Y[C]$ through a relation $\beta X[C] = dY/dC$,⁹ one obtains the formula

$$\chi_{IRM}(t + t_w, t_w) = Y[C(t + t_w, t_w)] - Y[C(t + t_w, 0)]. \quad (5)$$

The first term on the right is identified with the t_w -dependent TRM susceptibility.⁹ The second term corresponds to the TRM decay after zero waiting time. To avoid confusion, we shall refer to it as ZTRM, and drop the second argument. We will also use a corresponding observation time instead of a total age as the first argument of each function. For the ZTRM, the total age is equal to the observation time. Thus, Eq. (5) can be rewritten in the following form:

$$\chi_{IRM}(t, t_w) = \chi_{TRM}(t, t_w) - \chi_{ZTRM}(t + t_w). \quad (6)$$

The last formula expresses the well-known principle of superposition, which has been verified experimentally in the case of spin glasses.²³

It follows from Eq. (6) that the TRM relaxation is a superposition of two decays. The IRM is a response associated with the waiting time. The ZTRM is a response related to the cooling process. According to Eq. (5), it depends on $C(t + t_w, 0)$, which is a measure of the memory of the initial state. One can, in principle, consider an integral representation of the ZTRM:

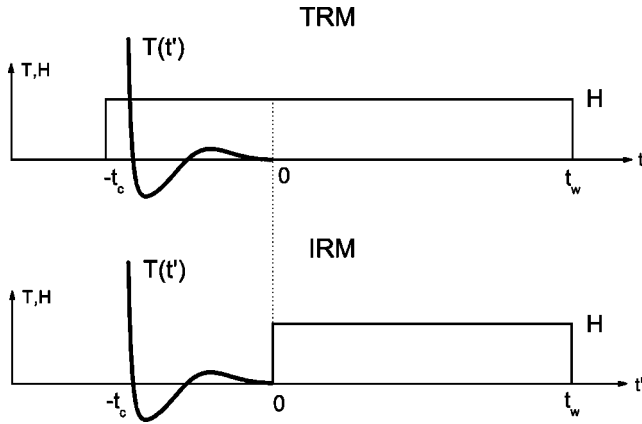


FIG. 1. Comparison of the TRM and the IRM (with $t_{w1}=0$ and $t_{w2}=t_w$) experimental protocols. The thick curve $T(t')$ denotes the temperature variation during a typical cooling process with an overall cooling time t_c . A magnetic field H is applied before the cooling in the TRM experiment, and immediately after the cooling in the IRM experiment.

$$\chi_{ZTRM}(t+t_w) = \int_{-t_c}^0 \tilde{R}[t+t_w, t', T(t')] dt', \quad (7)$$

where t_c is the overall cooling time. Unlike Eq. (4), the integrand in the last formula explicitly depends on temperature variation $T(t')$ during the cooling process. Therefore, a sum of the integral in Eq. (4) and the integral in Eq. (7) cannot be written as a single integral of the function $R(t+t_w, t')$ from $t' = -t_c$ to $t' = t_w$. This means that the thermal history cannot be taken into account by simple addition of the cooling time to the waiting time.

Figure 1 illustrates the difference between the TRM and the IRM experimental protocols. It also clarifies the meanings of t_w and t_c .

If the memory of the initial state is strong, there will be no one-to-one correspondence between the t_w -dependent correlation and t_w -dependent linear response. The TRM depends on the correlation $C(t+t_w, t_w)$, but it includes the response of the initial state. The IRM is a linear response, associated with the waiting time only, but it depends on the correlation with the initial state. Therefore, neither the TRM nor the IRM can be called a “true” t_w -dependent response.

The linear response theory predicts that the measured susceptibility [Eq. (4)] depends on the waiting time t_w . However, it gives no predictions regarding t/t_w scaling. Equation (6) suggests that the TRM and IRM, though characterized by the same waiting time, cannot have the same scaling properties. This is because they differ by the ZTRM, which is a one-time quantity without a characteristic time scale. Two exceptional cases are possible. First, the ZTRM decays so rapidly that the last term in Eq. (6) can be neglected for sufficiently large t_w . This case is usually considered in theoretical studies,^{2,9} which assume that memory of the initial condition is lost after very long waiting times, i.e., $C(t+t_w, 0) \rightarrow 0$ as $t_w \rightarrow \infty$.²⁴ Second, the ZTRM changes so slowly, that $\chi_{ZTRM}(t+t_w)$ for long enough t_w can be treated as a nonzero constant. This approach is similar to the treat-

ment of the field-cooled susceptibility, which is also a one-time quantity. We show in Sec. III B that neither of these two conditions holds in spin-glass experiments.

B. Analysis of t/t_w scaling

Spin-glass dynamics are characterized by at least two time scales. The microscopic attempt time τ_0 is associated with the quasiequilibrium decay at short observation times. The waiting time t_w determines the properties of the nonequilibrium relaxation at long times. Both types of spin-glass behavior have to be taken into account when the t/t_w scaling of the relaxation curves is analyzed.

Numerical studies of the off-equilibrium dynamics in the three-dimensional Edwards-Anderson model^{15,25} suggest that the autocorrelation function $C(t, t_w)$ can be well approximated by a product of two functions:

$$C(t, t_w) \propto t^{-\alpha} \Phi(t/t_w). \quad (8)$$

The waiting time independent factor $t^{-\alpha}$ represents the slow (on the logarithmic scale) quasiequilibrium decay at $t \ll t_w$. The function $\Phi(t/t_w)$ (which is approximately constant for $t \ll t_w$) describes the faster nonequilibrium relaxation at longer observation times. Of course, both α and $\Phi(x)$ depend on temperature.

A similar multiplicative ansatz²⁶ has been successfully used for scaling experimental TRM relaxation curves^{3,4}:

$$\chi_{TRM}(t, t_w) \propto t^{-\alpha} F(t_e/t_w^\mu). \quad (9)$$

Two features distinguish Eq. (9) from Eq. (8). First, an effective time t_e (usually denoted by λ) is introduced. The age of the system increases with the observation time as $t_w + t$, and the time/age ratio decreases. In order to allow a description of the relaxation by the same age t_w , the effective time should increase more slowly than the observation time t . This means that $dt_e/t_w = dt/(t+t_w)$ and $t_e = t_w \ln(1+t/t_w)$. Second, possible deviations from full t/t_w scaling in the aging regime are taken into account by the parameter μ . In this case, $dt_e/t_w^\mu = dt/(t+t_w)^\mu$, and the effective time is

$$t_e = t_w [(1+t/t_w)^{1-\mu} - 1]/(1-\mu). \quad (10)$$

At short observation times, $t \ll t_w$, the effective time is equivalent to the observation time: $t_e \approx t$.

The μ -scaling approach is very useful for studying departures from full t/t_w scaling, no matter whether μ itself has a clear physical meaning or not. We use this method in the present paper and determine μ from juxtaposition of relaxation curves, plotted versus t_e/t_w^μ .

A different method for separating the quasiequilibrium and aging regimes has also been successfully employed.² It is inspired by dynamical solution of mean-field models.¹⁰⁻¹² The following additive representation is considered²:

$$\chi_{TRM}(t, t_w) \propto A(t/\tau_0)^{-\alpha} + f(t_e/t_w^\mu). \quad (11)$$

This approach yields a better t/t_w scaling (μ closer to unity) than the previously discussed method.^{3,4} It should be noted, however, that derivation of the last formula² employs an assumption that $C(t+t_w, 0) = 0$. Therefore, Eq. (11) is exact

only asymptotically (large t_w), when long-term memory is weak. Nevertheless, this method is justified, because it gives good results on experimental time scales.

From a strict theoretical point of view, the μ -scaling analysis may be used only in the case of systems with one step of replica symmetry breaking. Indeed, for these systems, the aging part of the correlation function in the long-time limit can be written as^{10–12}

$$C_A(t+t_w, t_w) = j^{-1} [h(t+t_w)/h(t_w)], \quad (12)$$

where $h(t)$ is a monotonically increasing function. The μ -scaling approach corresponds to the following ansatz for this function^{2,10}:

$$h(t) = \exp[(t/\tau_0)^{1-\mu}/(1-\mu)]. \quad (13)$$

Systems with continuous replica symmetry breaking, such as the Sherrington-Kirkpatrick (SK) model, cannot be characterized by a single time scale in the aging regime, and Eq. (12) is not valid in this case.

Having said that, one should remember that experiments probe spin-glass dynamics only within limited time intervals, and the μ -scaling analysis works reasonably well in practice. Moreover, it is not clear which theoretical model is better suited for description of real spin glasses. Therefore, for practical purposes, we assume classification of departures from full t/t_w scaling based on the value of parameter μ . If $\mu < 1$, the apparent age of the spin-glass state increases more slowly than t_w , and spin-glass relaxation as a function of t/t_w is faster for longer waiting times. We shall refer to this behavior as “subaging.”² If $\mu > 1$, the apparent age grows faster than t_w , and relaxation plotted versus t/t_w is slower for longer waiting times. This behavior is called “superaging.”² The case of $\mu = 1$ corresponds to full t/t_w scaling.

III. EXPERIMENTAL RESULTS AND ANALYSIS

The purpose of this paper is to study how initial conditions affect aging phenomena in spin-glass experiments. By the initial condition we mean history of the spin-glass state before the waiting time begins. The initial conditions are always nontrivial in spin-glass experiments, because the quench, preceding the waiting time, is never infinitely fast.

All experiments were performed on a single crystal of Cu:Mn 1.5 at %, a typical Heisenberg spin glass with a glass temperature of about 15.2 K. The single crystal was used to avoid possible complications due to finite-size effects. Another advantage of this sample is its high de Almeida-Thouless (AT) critical line.²⁷ For example, the AT field at $T/T_g = 0.87$, the highest measurement temperature in our experiments, is about 600 Oe. This enables us to use a relatively large field change, $\Delta H = 10$ Oe, and still work well within the linear response regime. A commercial Quantum Design MPMS SQUID (superconducting quantum interference device) magnetometer was used for all the measurements. This equipment has been optimized for precision and reproducibility, rather than speed. Thus, cooling is relatively slow, and this allows us to study cooling effects in detail.

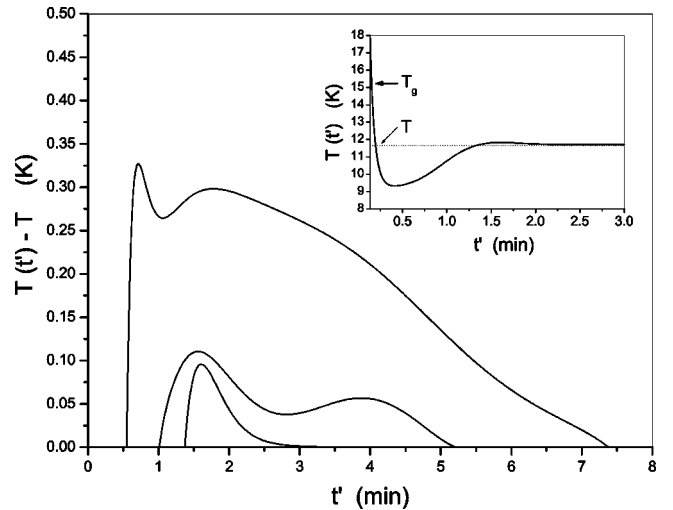


FIG. 2. Approach of the measurement temperature T during the cooling process. The temperature curves $T(t')$, from top to bottom, are for $T/T_g = 0.3, 0.4$, and 0.77 , respectively. The inset shows the whole cooling process for $T/T_g = 0.77$.

Some of the measurements have been repeated using Cryogenic S600 SQUID susceptometer, and yielded very similar results.

A. Cooling process and ZTRM

Spin-glass behavior is characterized by memory effects: properties of the measured spin-glass relaxation depend on history of a sample below T_g . The cooling process is an integral part of this history. It has been shown that, in real spin glasses, details of the experimental protocol well above the measurement temperature T do not affect the measured relaxation properties.¹⁹ However, the thermal history in the immediate vicinity of the measurement temperature (say, $\delta T < 0.5$ K) has a strong impact on the observed spin-glass behavior. This fact suggests that the cooling and waiting time effects cannot be separated and should be studied simultaneously.

A typical cooling protocol is exhibited in the inset of Fig. 2. The temperature drops rapidly to well below the measurement temperature, then rises to $T + \delta T$, and slowly approaches T from above. By definition, the experimental time starts when the measurement temperature T is finally reached.

The approach of the measurement temperature is shown in the main body of Fig. 2. For relatively high temperatures, $\delta T \approx 0.1$ K. For the lowest temperature, however, $\delta T \approx 0.3$ K. A comparison with the results of temperature cycling experiments¹⁹ suggests that the initial undercool is not very important, because of its large (several Kelvin) magnitude. The subsequent overshoot, however, may be expected to play a significant role in spin-glass dynamics, and cannot be neglected in our experiments.

A comment should be made at this point. Controlling a temperature protocol in real experiments is a difficult task. A spin-glass sample is cooled down together with a sample chamber, and the actual cooling process depends on the hardware. The temperature curves in Fig. 2 are not a matter of

choice. They are determined by the apparatus (in this case, Quantum Design MPMS), and cannot be modified easily. The present paper is devoted to conventional aging experiments, and the cooling process in Fig. 2 is very common indeed. It should also be noted that Fig. 2 exhibits temperature curves for helium gas, used as a heat transfer agent within the sample chamber. The actual temperature of the spin-glass sample lags behind. Therefore, in reality, the sample spends more time above the measurement temperature, than shown in Fig. 2. This makes the cooling effects stronger. Results of temperature cycling experiments¹⁹ suggest that a protocol, in which the sample is cooled down rapidly, and the measurement temperature is then approached from below without any overshoot, might reduce the cooling effects.

It is instructive to compare the cooling procedure in Fig. 2 with an experimental protocol including a positive temperature cycle.¹⁹ In this protocol, the sample is field cooled to the measurement temperature T , and kept for a long waiting time t_{w1} . Then it is heated up to $T + \delta T$ and annealed for a short time t_{w2} . After that, it is cooled down and kept at the initial temperature T for additional time t_{w3} . The field is then cut to zero, and the TRM relaxation is measured. It turns out that this relaxation follows a reference curve with $t_w = t_{w3}$ at short observation times, then breaks away and moves towards a reference curve with $t_w = t_{w1}$. Therefore, the spin-glass state initially exhibits a memory of only those events that happened after the temperature cycle. But, as time progresses, it begins to recall its earlier history. Another relevant analogy is an experimental protocol with a negative temperature shift after initial waiting.²⁰ In both experiments, the relaxation curve after the temperature change cannot be merged with any of the reference curves measured at a constant temperature.

The main idea of this paper is that any spin-glass aging experiment is, at the same time, a temperature variation experiment. All effects that manifest themselves in temperature variation experiments also appear in aging experiments.

Our reasoning is based on the hierarchical phase-space picture of spin-glass dynamics.^{19,20} In this picture, the spin-glass phase at temperatures below T_g is characterized by a large number of metastable states with hierarchical organization, similar to that of the pure equilibrium states in the SK model. These states are separated by free-energy barriers. As the temperature is lowered, the metastable states split in a hierarchical fashion, and the energy barriers grow. This process is reversed if temperature is raised. The hierarchical picture has been successfully used to explain results of temperature cycling experiments,^{19,20} as well as rejuvenation (chaoslike) and memory effects under a temperature change.²⁸

Let us consider a typical cooling process and imagine that the system spends some short time at a temperature $T + \delta T$. Several metastable states, separated by free-energy barriers, become populated during that time. As the temperature is lowered, these states split and produce new metastable states with new barriers. The old barriers grow steeply, and, for any value of the temperature there exist barriers diverging at this temperature.²¹ Therefore, when the measurement

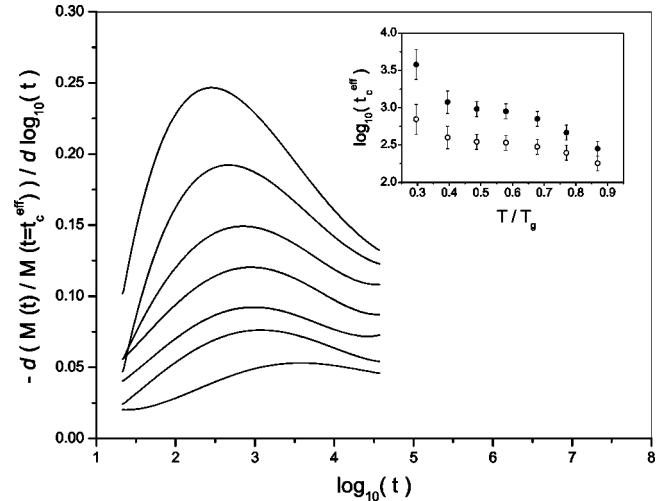


FIG. 3. The logarithmic relaxation rate for the ZTRM. The measurement temperatures, from top to bottom, are $T/T_g = 0.87, 0.77, 0.68, 0.58, 0.5, 0.4$, and 0.3 . The inset shows the temperature dependence of logarithms of the effective cooling time t_c^{eff} (solid symbols) and the effective scaling time t_s^{eff} (open symbols).

temperature T is finally reached, there is a large number of metastable states, separated by barriers of all heights.²⁹ In other words, the cooling process creates an initial state with a broad spectrum of relaxation times. This situation corresponds to the “existence of domains of all sizes within the initial condition” in the real-space picture.²⁸

If a waiting time t_w follows the cooling, properties of the subsequent relaxation will be similar to those in the positive temperature cycle experiment. At short observation times, the relaxation will be governed by t_w . At longer observation times, it will break away and slow down, because the long-time metastable states with high barriers, created by the cooling process, will come into play. This effect will be more pronounced after shorter waiting times.

Properties of the initial state, produced by the cooling process, can be studied by measuring a TRM decay for $t_w = 0$, which we call ZTRM. The sample is cooled down in the presence of a small field, $H = 10 Oe$. When the temperature is stabilized, the field is cut to zero, and decay of the ZTRM is recorded.

Figure 3 exhibits logarithmic relaxation rates of this decay, corresponding to different temperatures. The experimental ZTRM curves were fitted using a five-order polynomial fit, and then differentiated with respect to $\log_{10}(t)$. Each curve in Fig. 3 has a peak, and we shall call the position of this peak the “effective cooling time” t_c^{eff} . Each ZTRM curve is normalized by 1 at $t = t_c^{eff}$ before differentiation is performed. It can be seen from Fig. 3 that the peaks become much broader as the temperature decreases. This means that the spectrum of relaxation times broadens as well, and that it is not dominated by a single time scale.

Even though the effective cooling time t_c^{eff} corresponds to the maximum of the relaxation rate, it cannot be treated as a regular waiting time t_w . We have tried to scale each ZTRM curve with the relaxation curves for longer waiting times, using the μ -scaling approach and taking t_c^{eff} as the scaling

parameter. No value of μ can give even an approximate scaling, especially at short times. It turns out, however, that the ZTRM curve for any temperature can be merged with the other TRM curves (using the same μ as used for the longer waiting times), if a much shorter characteristic time for the ZTRM is introduced. We call this time the “effective scaling time” t_s^{eff} . It is several times shorter than the effective cooling time. The inset of Fig. 3 exhibits logarithms of t_c^{eff} and t_s^{eff} for different temperatures.

The fact that one can consider at least two characteristic times for the ZTRM agrees with what is expected from relaxation in the positive-temperature-cycle experiment. The spin-glass behavior at short observation times is governed by t_s^{eff} , which can be associated with ordinary aging effects during the slow asymptotic approach of the measurement temperature. However, the long-time relaxation is strongly influenced by the metastable states, separated by high barriers, resulting from the temperature change. Thus, the relaxation rate peaks at t_c^{eff} , and not at t_s^{eff} .

This argument can be generalized to include the TRM experiments with longer waiting times. The logarithmic relaxation rate has a peak at t_w^{eff} , the “effective waiting time.” It is well known that t_w^{eff} for the TRM is greater than t_w .²² We believe that this shift in the maximum of the relaxation rate is caused by those long-time metastable states, which are created during the cooling process.

It is important to note that the memory of the initial state depends not only on the cooling protocol, but also on the overall complexity of the free-energy landscape. This can be illustrated by measurements of the ZTRM in the presence of a high constant field. The minimum possible overlap, $q_{min}(H)$, between two states increases with increasing magnetic field H .³⁰ Therefore, certain constraints on barrier heights are imposed by the field, leading to a faster relaxation. The experiment is performed in the following way. First, the sample is cooled down to the measurement temperature at the field $H + \Delta H$. The field is changed to H , and the ZTRM, is measured for some time. Second, the sample is warmed up to above T_g , and cooled down again, all in the presence of the same field H . The field-cooled magnetization (MFC) is measured for the same time. The difference of these two magnetizations is then fitted to a power law at long observation times: $ZTRM(t, H, \Delta H) - MFC(t, H) \propto t^{-\lambda(H)}$. The values of H were varied from 50 to 1000 Oe. The field change was small, $\Delta H = 10$ Oe, so that the response was always linear.

Figure 4 exhibits the measured ZTRM and MFC decays for $H = 500$ Oe. One can see that time dependence of the MFC cannot be neglected at high fields. The inset shows the relaxation exponent $\lambda(H)$. The exponent appears to be a linear function of $q_{min} \propto H^{2/3}$. This is not surprising, because its temperature dependence is also close to linear, and the AT critical line, $T_g - T_c(H) \propto H^{2/3}$, has a profound effect on spin-glass dynamics.²⁷ The estimated value of $\lambda(H)$ near the AT line, which corresponds to $H_{AT} \sim 1400$ Oe at this temperature, is 0.27 ± 0.03 . It is interesting that this number compares well with the Monte Carlo result, $\lambda \approx 0.25$, for the three-dimensional Edwards-Anderson (3D EA) model at zero magnetic field.²⁵

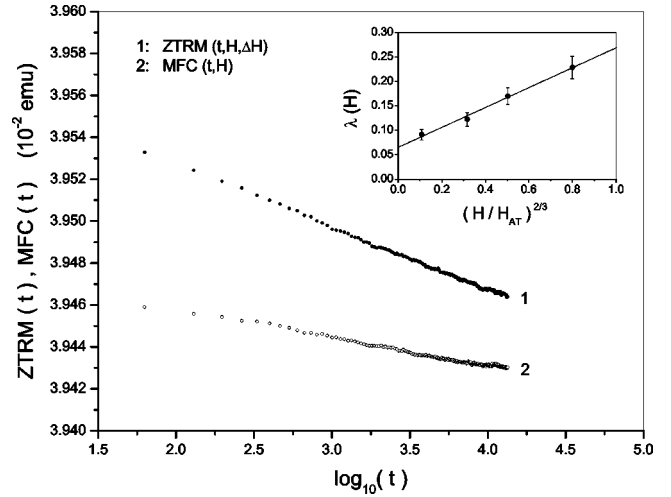


FIG. 4. Time dependences of the ZTRM and MFC, measured at $T/T_g = 0.79$ and $H = 500$ Oe. The field change is $\Delta H = 10$ Oe. The inset shows the relaxation exponent $\lambda(H)$ as a function of $H^{2/3}$.

The observed increase in $\lambda(H)$ suggests that energy barriers, created by the cooling process, are lower, if cooling is performed in the presence of a high field. This happens, because the accessible phase space is limited by $q_{min}(H)$. The low-field initial state in our experiments appears to be more complex, i.e., characterized by higher barriers, than the initial state in the Monte Carlo simulations.

B. Comparison of the TRM and the IRM

It was shown in Sec. II A that the TRM relaxation can be decomposed into a sum of two decays: the IRM, which is a response of the system during the waiting time t_w , and the ZTRM, which is a response of the initial state.

Figure 5 displays the experimental TRM and ZTRM curves, and their difference, for $T/T_g = 0.87$ and t_w

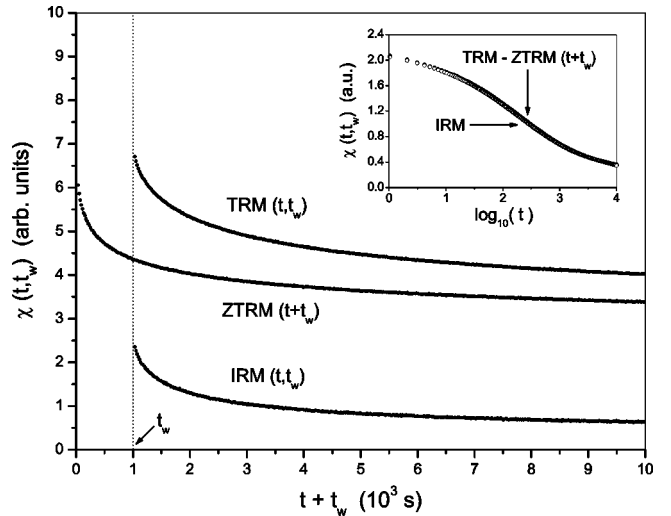


FIG. 5. Experimental time dependence of the $\chi_{TRM}(t, t_w)$ and $\chi_{IRM}(t, t_w)$ for $T/T_g = 0.87$ and $t_w = 1000$ s. The TRM relaxation for zero waiting time is referred to as ZTRM. The inset illustrates the validity of the principle of superposition.

=1000 s. The inset of Fig. 5 demonstrates that the measured IRM is equivalent to the difference of the separately measured TRM and ZTRM (the waiting time for data in the inset is 300 s). One can see from Fig. 5 that the response of the initial state dominates the measured TRM relaxation. This effect is particularly pronounced at low temperatures, at which thermally activated processes are slow. Figure 5 suggests that the ZTRM cannot be neglected, nor can it be treated as a constant. Therefore, the TRM and IRM relaxation curves will have different scaling properties, and should be analyzed simultaneously.

The correlation function $C(t+t_w, t_w)$, defined by Eq. (1), is independent of t_w at $t=0$. Numerical studies of the SK model demonstrate^{31,32} that the correlation curves for different waiting times, plotted versus t/t_w , cross at one point, corresponding to $t \approx t_w$. This is a consequence of dynamic ultrametricity. Because a time scale is associated with each value of the correlation, there exists a value of C , such that $t(C) = t_w$. If the linear response susceptibility depends on its time arguments only through the correlation function, i.e. $\chi = \chi(C)$, the susceptibility curves should also cross at one point. Experimental results do not exhibit this property. The TRM curves for long waiting times lie below the curves for short waiting times, when plotted vs t/t_w . The IRM curves demonstrate the opposite behavior.

In the present paper, we normalize both the TRM and IRM decays by 1 at $t=t_w$, and treat them as “normal” relaxation functions. This approach has several advantages. First, all departures from full t/t_w scaling, reflected in the shapes of relaxation curves, can be observed clearly. Second, the shapes of TRM and IRM decays can be compared in detail, regardless of the fact that their magnitudes are different. Third, experimental results can be directly compared with results of numerical simulations. We believe that this approach is physically justified because the influence of the cooling process leads to systematic changes in the *shapes* of relaxation curves, as discussed in Sec. III A. This method is different from the one, traditionally used to study t/t_w scaling.^{2,3}

Figure 6 exhibits the TRM and IRM relaxation curves, measured at $T/T_g = 0.87$, for two waiting times, $t_w = 1000$ and 6310 s. The TRM data demonstrate the familiar subaging pattern: the relaxation, plotted versus t/t_w , is faster for the longer waiting time. The IRM results show a quite different behavior: the relaxation as a function of t/t_w slows down as t_w increases. This is the superaging.

In order to make the above conclusion quantitative, we analyze the t/t_w scaling of measured relaxation curves using the μ -scaling approach, discussed in Sec. II B. We optimize μ to achieve the best possible scaling over a wide range of observation times, with particular attention to the aging regime, $t > t_w$. Inclusion of the quasiequilibrium decay with the exponent α improves scaling at short times, but it does not help at longer times. In the present analysis, the quasiequilibrium behavior is not taken into account explicitly. This gives values of μ a little further from unity, but does not affect any conclusions about scaling in the aging regime.

Figure 7 exhibits values of the parameter μ for the TRM and IRM. In the case of the TRM, μ lies between 0.8 and 0.9

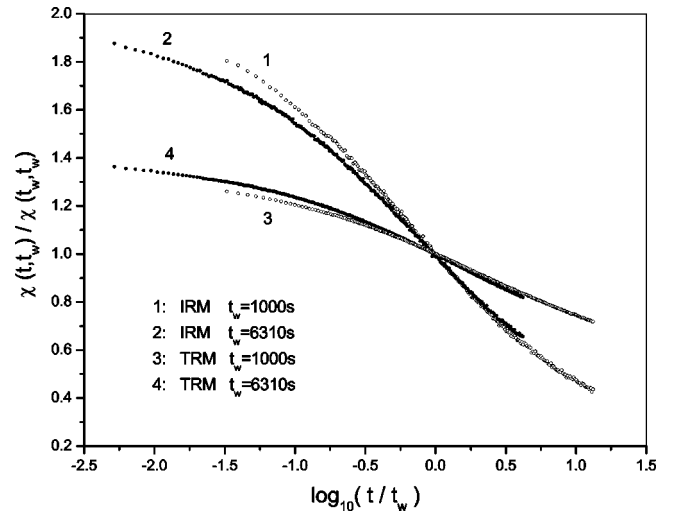


FIG. 6. Relaxation curves $\chi_{IRM}(t, t_w)$ and $\chi_{TRM}(t, t_w)$ for two waiting times, normalized by 1 at $t=t_w$. The temperature is $T/T_g = 0.87$. The IRM decay as a function of t/t_w is slower for longer waiting times (“superaging”). The TRM decay is faster for longer waiting times (“subaging”).

for relatively high temperatures, but drops visibly at low temperatures, $T/T_g < 0.4$. Similar results have been obtained for various spin-glass samples.²⁻⁴

The values of μ for the IRM are greater than unity. They are near 1.1, but tend to increase at low temperatures. According to Fig. 7, there is a certain symmetry with respect to $\mu = 1$ between the values of μ for the TRM and IRM.

Figure 8 exhibits values of logarithm of the effective waiting time t_w^{eff} for these two functions. The relaxation curves were fitted using a five-order polynomial fit, and then differentiated with respect to $\log_{10}(t)$. The effective waiting time t_w^{eff} corresponds to the extremum of this derivative. It can be seen from Fig. 8 that $t_w^{eff} > t_w$ for the TRM, but $t_w^{eff} < t_w$ for

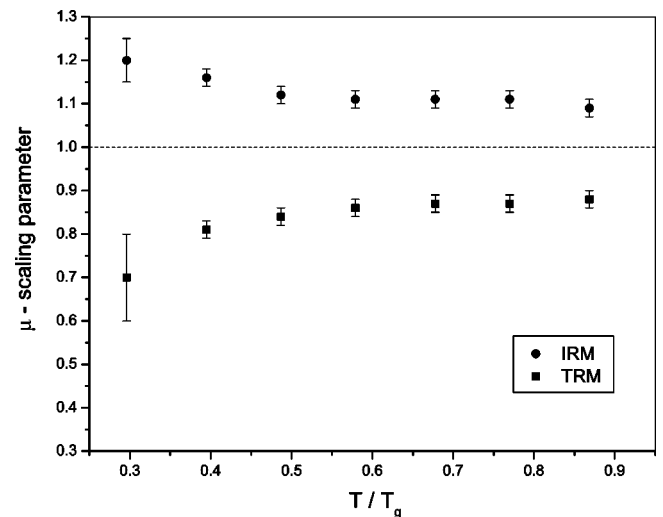


FIG. 7. The scaling parameter μ as a function of temperature obtained by scaling together relaxation curves for $t_w = 6310$ and 1000 s. Note that $\mu > 1$ for the IRM (“superaging”), and $\mu < 1$ for the TRM (“subaging”).

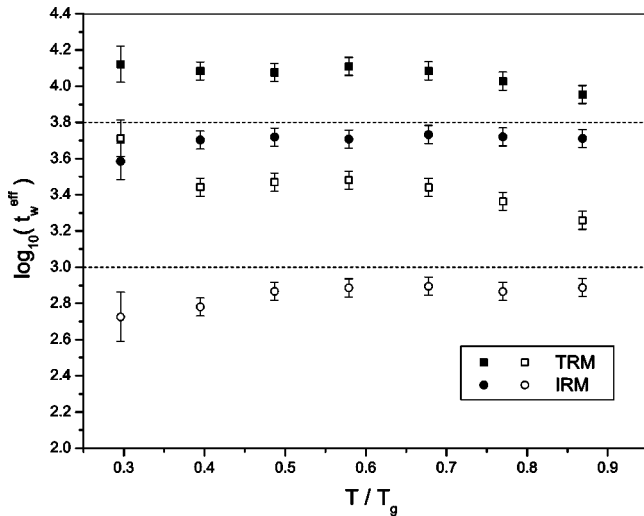


FIG. 8. Logarithm of the effective waiting time, t_w^{eff} , as a function of temperature. The solid symbols correspond to $t_w=6310$ s, and the open symbols to $t_w=1000$ s. Note that $t_w^{eff} > t_w$ for the TRM, and $t_w^{eff} < t_w$ for the IRM.

the IRM. While the first of these inequalities is well known, the last inequality represents a new and somewhat unexpected result.

Figure 9 displays values of the relaxation exponent, $\lambda(T, t_w)$, defined through $\chi(t, t_w) \propto t^{-\lambda(T, t_w)}$ for $t \gg t_w$. This definition is based on the fact that time dependence of spin-glass relaxation is essentially algebraic in the aging regime.^{8,9,15,25} The value of $\lambda(T, t_w)$ is determined from the slope of the linear fit to $\log_{10}(\chi)$ as a function of $\log_{10}(t)$. Because of time limitations in our experiments, the fitting was performed in the interval $t/t_w=1.5 \dots 10$ for t_w

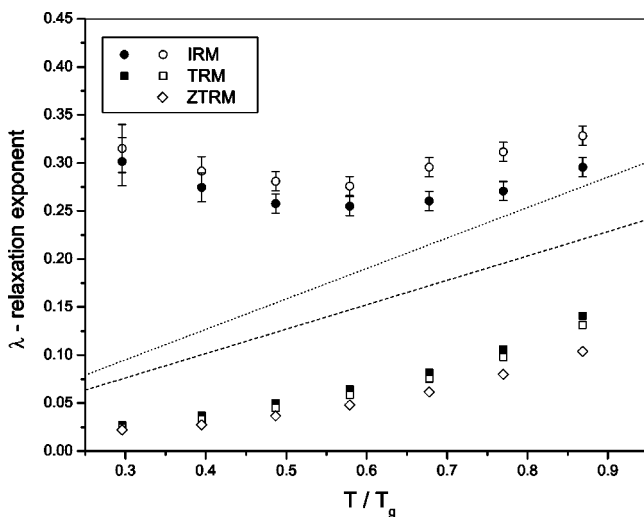


FIG. 9. The relaxation exponent $\lambda(T, t_w)$ as a function of temperature. The solid symbols correspond to $t_w=6310$ s, and the open symbols to $t_w=1000$ s. The open diamonds denote λ for the experimental ZTRM. The error bars in the case of TRM and ZTRM are smaller than the symbol sizes. The upper and lower straight lines are Monte Carlo results for $t_w=0$ and 1000 mcs, respectively (see the text).

$=1000$ s, and in the interval $t/t_w=1.5 \dots 5$ for $t_w=6310$ s. In the case of the ZTRM, the effective cooling time, t_c^{eff} , was used instead of t_w .

The first conclusion one can draw from Fig. 9 is that the ZTRM is the *slowest* relaxation measured in the aging regime. This result is in sharp contradiction with results of numerical simulations, which show that the zero waiting time decay is the *fastest* possible relaxation. The dotted (upper) line in Fig. 9 represents $\lambda(T)$ for $t_w=0$ from the Monte Carlo studies of the 3D EA model of Kisker *et al.*²⁵ Our experimental values of the $\lambda(T)$ for the ZTRM are about three times lower.

According to Fig. 9, the TRM decay as a function of t/t_w becomes faster as the waiting time increases, while the IRM relaxation becomes slower. The corresponding values of $\lambda(T, t_w)$ move towards each other and towards the dashed (lower) line, which represents numerical results for the EA model with $t_w=1000$ mcs.²⁵ This observation suggests that the exponent λ for the ideal (i.e. free from cooling effects) spin-glass relaxation should take values somewhere in between those for the TRM and IRM.

C. Discussion

The phenomenon of superaging may seem rather unusual from an experimentalist's point of view, because it has never been observed in TRM experiments. It turns out, however, that this is a predominant effect in Monte Carlo simulations. For example, Fig. 4 in Marinari *et al.*,³¹ Fig. 4 in Takayama *et al.*,³² and Fig. 4 in Cugliandolo *et al.*³³ demonstrate dynamic behaviors, very similar to superaging. In all these simulations of the SK model, the correlation function $C(t + t_w, t_w)$, plotted versus t/t_w , decays slower for longer waiting times. This would correspond to $\mu > 1$. However, as mentioned in Sec. II B, the μ -scaling analysis cannot be expected to work equally well for all time scales in a system with continuous replica symmetry breaking.

In the case of the 3D EA model, it is difficult to distinguish between the subaging and superaging effects, because the correlation curves exhibit good t/t_w scaling in the aging regime.^{15,25} However, there may be a slight tendency towards superaging, as suggested by Fig. 2 in Kisker *et al.*²⁵ In four dimensions, the correlation function of the EA model after an infinitely fast quench exhibits the superaging with $\mu=1.05$ according to Fig. 4 in Berthier and Bouchaud.³⁴ However, it becomes subaging with $\mu=0.96$ after a slow cooling.³⁴ One of the conclusions reached by these two authors is that "a finite cooling rate effect . . . leads to an apparent sub-aging behavior for the correlation function, instead of the superaging that holds for an infinitely fast quench."³⁴

Numerical simulations of 3D Heisenberg spin glasses also reveal the subaging/superaging ambiguity. The spin autocorrelation function exhibits subaging in the fully isotropic case, according to Fig. 2 in the work by Kawamura,³⁵ but becomes clearly superaging in the presence of even weak anisotropy (Fig. 4 there).

All these results suggest that it is the superaging, and not the subaging, that may be the "natural" scaling behavior. However, any comparison of experimental and numerical

data should be made with caution, because conventional aging experiments measure response functions, while Monte Carlo simulations usually study only correlations.

Appearance of the subaging in a typical TRM experiment can be explained as follows. When the cooling is over, a number of metastable states, separated by free-energy barriers of different heights, are already populated. We shall refer to them loosely as the initial state. The response of this state, the ZTRM, is slow and cannot be characterized by a single well-defined time scale. The initial state is not random: it has already evolved towards some equilibrium state, and this makes it energetically favorable. During the waiting time, evolution continues in the same direction. Thus, aging and cooling effects work together, and the spin-glass state appears to be older. The characteristic barrier is higher than $\Delta(T, t_w) = k_B T \ln(t_w/\tau_0)$, the barrier associated with the waiting time t_w .²⁰ The TRM decay is slower than the ideal t_w -dependent relaxation, which can be characterized by some exponent λ_0 . However, as the waiting time increases, influence of the initial condition diminishes. The TRM relaxation, plotted versus t/t_w , becomes faster, and its dependence on t_w stronger. This leads to the subaging behavior with $\mu < 1$, $t_w^{eff} > t_w$, and $\lambda < \lambda_0$.

Presence of many metastable states, separated by high barriers, is a well-known problem in Monte Carlo simulations, involving thermalization of large samples. The system easily gets trapped in a metastable state and cannot efficiently explore the entire phase space to find the ground state.³⁶ The cooling process in spin-glass experiments gives a similar result: the system is trapped before the waiting time begins. However, Monte Carlo studies of aging phenomena do not typically simulate the cooling protocol. The simulations are started directly at the measurement temperature from a random initial configuration, and results are averaged over different initial conditions. This may be the reason why the subaging behavior is not normally observed in numerical simulations. Moreover, the random initial configuration corresponds to zero net magnetization. This means that Monte Carlo studies are probably closer to the IRM, than to the

TRM, experiments.³³ The difference between the two is not very important, if memory of the initial state disappears quickly. This, however, is not the case in real spin glasses.

The above arguments provide a consistent explanation for the subaging behavior of the TRM, but they are insufficient to explain scaling properties of the IRM. Indeed, Figs. 7, 8, and 9 suggest that parameters μ , t_w^{eff} , and λ for the IRM relaxation are temperature dependent, though to a lesser extent, than in the case of the TRM. This means that subtraction of the ZTRM does not completely eliminate effects of the cooling process. There is no doubt that the IRM is closer to the ideal (i.e., independent of cooling effects) response function, than the TRM. However, our experimental data do not give a clear answer to the question about scaling properties of this ideal function. In particular, we cannot exclude the possibility that it might exhibit full t/t_w scaling.

IV. CONCLUSION

In this paper, we study the influence of initial conditions on t/t_w scaling properties of spin-glass relaxation. We argue that the initial condition for aging, created by the cooling process, is not random, and characterized by a broad distribution of time scales. As a result, the TRM decay, measured in spin-glass experiments, is dominated by the response of the initial state. Subtraction of this response according to the principle of superposition leads to a qualitatively different scaling behavior for the IRM. While the TRM has the well-known subaging properties, the IRM exhibits superaging. To our knowledge, this is the first observation of superaging in spin-glass experiments. A comparison with results of numerical simulations suggests that it is the superaging, and not the subaging, that may be the “natural” scaling behavior in spin-glass dynamics.

ACKNOWLEDGMENT

We are most grateful to Professor J. A. Mydosh for providing us with the Cu:Mn single crystal sample, prepared in Kamerlingh Onnes Laboratory (Leiden, The Netherlands).

¹L. Lundgren, P. Svedlindh, P. Nordblad, and O. Beckman, Phys. Rev. Lett. **51**, 911 (1983).

²E. Vincent, J. Hammann, M. Ocio, J.-P. Bouchaud, and L.F. Cugliandolo, in *Complex Behavior of Glassy Systems*, edited by M. Rubi, Springer Verlag Lecture Notes in Physics, Vol. 492 (Springer-Verlag, Berlin, 1997). Available as cond-mat/9607224.

³M. Ocio, M. Alba, and J. Hammann, J. Phys. (France) Lett. **46**, L1101 (1985); M. Alba, M. Ocio, and J. Hammann, **2**, 45 (1986).

⁴M. Alba, J. Hammann, M. Ocio, and Ph. Refregier, J. Appl. Phys. **61**, 3683 (1987).

⁵L.C.E. Struik, *Physical Aging in Amorphous Polymers and Other Materials* (Elsevier, Houston, 1978).

⁶J.-P. Bouchaud, E. Vincent, and J. Hammann, J. Phys. I **4**, 139 (1994).

⁷B. Rinn, P. Maass, and J.-P. Bouchaud, Phys. Rev. Lett. **84**, 5403

(2000).

⁸J.-P. Bouchaud, J. Phys. I **2**, 1705 (1992).

⁹J.-P. Bouchaud and D.S. Dean, J. Phys. I **5**, 265 (1995).

¹⁰J.-P. Bouchaud, L. F. Cugliandolo, J. Kurchan, and M. Mezard, in *Spin Glasses and Random Fields*, edited by A.P. Young (World Scientific, Singapore, 1997).

¹¹L.F. Cugliandolo and J. Kurchan, Phys. Rev. Lett. **71**, 173 (1993).

¹²L.F. Cugliandolo and J. Kurchan, J. Phys. A **27**, 5749 (1994).

¹³L.F. Cugliandolo and J. Kurchan, Phys. Rev. B **60**, 922 (1999).

¹⁴D.S. Fisher and D.A. Huse, Phys. Rev. B **38**, 373 (1988); **38**, 386 (1988).

¹⁵H. Rieger, J. Phys. A **26**, L615 (1993); Physica A **224**, 267 (1996).

¹⁶L.L. Bonilla, F.G. Padilla, and F. Ritort, Physica A **250**, 315 (1998); C. Godreche and J.M. Luck, J. Phys. A **29**, 1915 (1996).

¹⁷L. Berthier, Eur. Phys. J. B **17**, 689 (2000).

¹⁸We do not consider a quench from a high magnetic field here. For

- details, see P. Nordblad, P. Svedlindh, P. Granberg, and L. Lundgren, *Phys. Rev. B* **35**, 7150 (1987); F. Lefloch, J. Hammann, M. Ocio, and E. Vincent, *Physica B* **203**, 63 (1994).
- ¹⁹Ph. Refregier, E. Vincent, J. Hammann, and M. Ocio, *J. Phys. I* **48**, 1533 (1987).
- ²⁰M. Lederman, R. Orbach, J.M. Hammann, M. Ocio, and E. Vincent, *Phys. Rev. B* **44**, 7403 (1991).
- ²¹J. Hammann, M. Ocio, E. Vincent, M. Lederman, and R. Orbach, *J. Magn. Magn. Mater.* **104**, 1617 (1992).
- ²²K. Jonason and P. Nordblad, *Physica B* **279**, 334 (2000).
- ²³L. Lundgren, P. Nordblad, and L. Sandlund, *Europhys. Lett.* **1**, 529 (1986).
- ²⁴S. Franz and H. Rieger, *J. Stat. Phys.* **79**, 749 (1995).
- ²⁵J. Kisker, L. Santen, M. Schreckenberg, and H. Rieger, *Phys. Rev. B* **53**, 6418 (1996).
- ²⁶Note that a comprehensive description of results from magnetic noise, relaxation, and susceptibility measurements suggests that a quasiequilibrium factor ($t^{-\alpha} + \delta$), where δ is a constant, should be used instead of $t^{-\alpha}$, as explained in Ref. 4 above.
- ²⁷V.S. Zotev, G.G. Kenning, and R. Orbach, *Phys. Rev. B* **66**, 014412 (2002).
- ²⁸K. Jonason, P. Nordblad, E. Vincent, J. Hammann, and J.-P. Bouchaud, *Eur. Phys. J. B* **13**, 99 (2000).
- ²⁹Note that the experimental data suggesting divergence of free-energy barriers at any temperature below T_g can be reanalyzed in terms of barriers, that vanish at T_g , and remain finite at lower temperatures. See J.-P. Bouchaud, V. Dupuis, J. Hammann, and E. Vincent, *Phys. Rev. B* **65**, 024439 (2002). The barriers, nevertheless, grow with decreasing temperature.
- ³⁰G. Parisi, *Phys. Rev. Lett.* **50**, 1946 (1983); *Physica A* **124**, 523 (1984).
- ³¹E. Marinari, G. Parisi, and D. Rossetti, *Eur. Phys. J. B* **2**, 495 (1998).
- ³²H. Takayama, H. Yoshino, and K. Hukushima, *J. Phys. A* **30**, 3891 (1997).
- ³³L.F. Cugliandolo, J. Kurchan, and F. Ritort, *Phys. Rev. B* **49**, 6331 (1994).
- ³⁴L. Berthier and J.-P. Bouchaud, *Phys. Rev. B* **66**, 054404 (2002).
- ³⁵H. Kawamura, *Phys. Rev. Lett.* **80**, 5421 (1998).
- ³⁶E. Marinari, G. Parisi, F. Ricci-Tersenghi, and F. Zuliani, *J. Phys. A* **34**, 383 (2001).